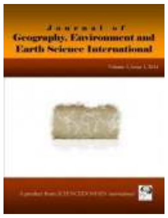

Journal of Geography, Environment and Earth Science International

9(3): 1-14, 2017; Article no.JGEESI.32086

ISSN: 2454-7352

SCIENCEDOMAIN *international*

www.sciencedomain.org

Shoreline Change Rate Detection and Future Prediction Using Remote Sensing and GIS Techniques: A Case Study of Ras EL-Hekma, North Western Coast, Egypt

M. E. Basiouny[1], S. B. El Kafrawy[2], E. A. Ghanem[3] and A. S. Taha[3*]

[1]Department of Civil Engineering, Faculty of Engineering, Egyptian Chinese University (ECU), Egypt.

[2]Department of Marine Sciences, National Authority for Remote Sensing and Space Sciences (NARSS), Egypt.

[3]Department of Civil Engineering, Benha Faculty of Engineering, Benha University, Egypt.

Authors' contributions

This work was carried out in collaboration between all authors. All authors participated equally in the study idea, literature review, data collection and analyses, methodology, statistical analyses, tabulating the data, results validation, writing and revising the whole manuscript. All authors read and approved the final manuscript.

Article Information

DOI: 10.9734/JGEESI/2017/32086

Editor(s):

(1) Mohamed Nageeb Rashed, Department of Chemistry, Aswan University, Egypt.

Reviewers:

(1) Edward Ching-Ruey, Luo, National Chi-nan University, Taiwan.

(2) Ali Atef Yousef Ali, Mansoura university, Egypt.

Complete Peer review History: http://www.sciencedomain.org/review-history/18320

Case Study

Received 7th February 2017
Accepted 4th March 2017
Published 24th March 2017

ABSTRACT

Shoreline mapping and change rate along the Ras El-Hekma, north west of Egypt has been analyzed. Thresholding band ratio method, in which a thresholding value is selected either by man-machine interaction or by a local adaptive strategy, has been used to extract shoreline. Digital Shoreline Analysis System (DSAS) used to detect Change rate of shorelines by EPR (end point rate model). Also future shoreline positions based on precedent shorelines has been predicted and has been corrected. Rates and trends Information of shoreline change can give

**Corresponding author: E-mail: ahmedo354@yahoo.com;*

recommendation to the decision makers to decide the best coastal area to be invested and also can be used to improve understanding of underlying causes and potential effects of coastal erosion/ accretion which can support informed coastal management. Multi-temporal satellite images acquired from (USGS) U.S. Geological Survey in 1973, 1987, 1995,2003 and 2015 along time period 42 years. These images were used to detect the shoreline position, predict the future shoreline, and to estimate change rate. The results show that the eastern side of study area tends to erosion all the time period. The western area has about 40- 70% erosion and 30-60% accretion depend on date. Overall 42 years the maximum accretion rate is 12 m/year and erosion rate is -9.65m/year. The average rates are defined from -0.8 to -4.25 for erosion and 0.05 to 1.60 for accretion definitely not high. The predicted shoreline was compared with the actual shoreline detected from high resolution satellite imagery of 2015. The positional shift at each sample point is observed. The positional error varies from -49.8 m to 76.3 m. The Rote Mean Square Error (RMSE) for the future predicted shoreline2015 was found to be 15.75 m. also 2020and 2050 shorelines has been predicted and corrected.

Keywords: Shoreline change rate; shoreline prediction; thresholding band ratio; end point rate; ras El-Hekma.

1. INTRODUCTION

Early dates from 1807 to 1927, all shoreline maps have been generated by ground surveying. From 1927 to 1980, aerial photographs were known as a unique source for a coastal mapping. However, the number of aerial photographs required for shoreline mapping, even at a regional scale, is large [1]. Collecting, analyzing and transferring the information from photographs to the map are exorbitant and time-consuming. Also, the black and white photographs create many problems. 1) The contrast between the land and water in spectral range of panchromatic photographs is minimal, mainly for turbid or muddy water of coastal zone, and the detection of shoreline is difficult [2]. 2) Photographs and resultant maps are in a non-digital format, dipping versatility of data set. A complex process is necessary to transfer information to the digital format, which introduces extra costs and errors. The geometric complexity and fragmented patterns of shorelines compounds these problems. In addition to previous, other possible limitations are: a) lack of timely coverage, (2) lack of geometrical accuracy unless ortho-rectified, (3) the expense of the analytical equipment, (4) the intensive nature of the procedure [3], and (5) the need for skilled personnel. In addition to high costs and difficulties, generation of shoreline maps has fallen sadly out of date. From 1972 Landsat and another remote sensing satellite provide digital imagery in infrared spectral bands where the land-water interface is well defined. Hence remote sensing imagery and image processing techniques provide a possible solution to some of the problems of generating and updating the shoreline maps [4]. Coastal zone has an important effect in countries' economic. Coastal zones monitoring are an important task in environmental protection and sustainable development. For example, it may be used for construction, Water desalination plants, Electrical power generation stations and Sewage treatment plants etc. Coastal zones are very weak and dynamic according to both human disturbances and natural [5]. Also it has a high dynamic environment with many physical processes such as sea level rise, tidal flooding, land subsidence, and erosion-sedimentation. Those factors play important role in change position of shoreline and development of coastal landscape. Mediterranean Sea connects both Africa and Europe, and it is one of the most Guyana and complex ecosystems on Earth. Egypt is one of countries overlooking Mediterranean Sea, where Egypt has a shoreline with a length about 1300 kilometers stretches eastward from Egyptian Rafah even the far west Salloum that is showing how importance for studying the coastal area. Ras El-Hekma is concerned of the promising area of the Mediterranean regions where it was recently launched tourism investment by Egyptian government. The main objective of the recent study is to investigate the erosion/accretion area and shoreline change rate over time in study area. Also, future shoreline positions have been predicted along near time and far, ranging from 5 years to 35 years, to help decision maker in monitoring a coastal area of Ras El- Hekma. The model of future shoreline prediction has been validated and then future shoreline corrected.

2. MATERIALS AND METHODS

2.1 Study Area

Study site of this investigation is RAS El-Hekma, northwest of Egypt. These coastal zones receive attention by Egyptian government because it is most promising area for future of tourism investment to Egypt during the coming 20 years, flows of funds and foreign direct investment estimated at tens of millions of dollars in capital . This coastal area stretching from Dabaa area in Kilo 170 by way of the northwest coast to the km 220 in Matrouh, along with about 58 km. It is surrounded in the north by Mediterranean Sea and in the south by the west desert of Egypt. Ras El-Hekma is located in the northwest of Egypt, Geographic coordinates range from 31° 6 ` N to 31°15 ` N in latitude and 27°41 ` E to 27°53 ` E in longitude. Fig. 1 is showing study area.

2.2 Satellite Data

The image data was acquired at unequal intervals between 1973 and 2015, covering a time span of 42 years. All images in good quality and have no clouds effect. To extract and determine changes along shoreline of Ras El-Hekma, six satellite images were utilized five from Landsat: one from the Landsat MSS (60 m spatial resolution) acquired in May, 1973, three from the Landsat-5 TM (30 m spatial resolution) acquired in August 1987, July 1995 and August 2003and one from the Landsat-8 OLI_TIRS(30 m spatial resolution) acquired in August, 2015 and another one as a reference map from Pleiades-1B (0.50 m spatial resolution) acquired in August, 2015. Landsat MSS image of 1973 has been resampled to 30m to match the spatial resolution of Landsat TM-5 images of 1987, 1995, 2003, and OLI_TIRS 2015. All the data sets are projected in UTM projection with zone no 35 and WGS 84 datum. All images are rectified by United States geology surveying (USGS) with total root mean square error (RMSE) less than 0.44 m.

2.3 Image Pre-Processing

2.3.1 Geometric correction

The objective of geometric correction of the image is to rectify the distortions introduced by relief, atmospheric refraction, earth curvature and nonlinearities of the sensor's instantaneous field of view. While many researchers

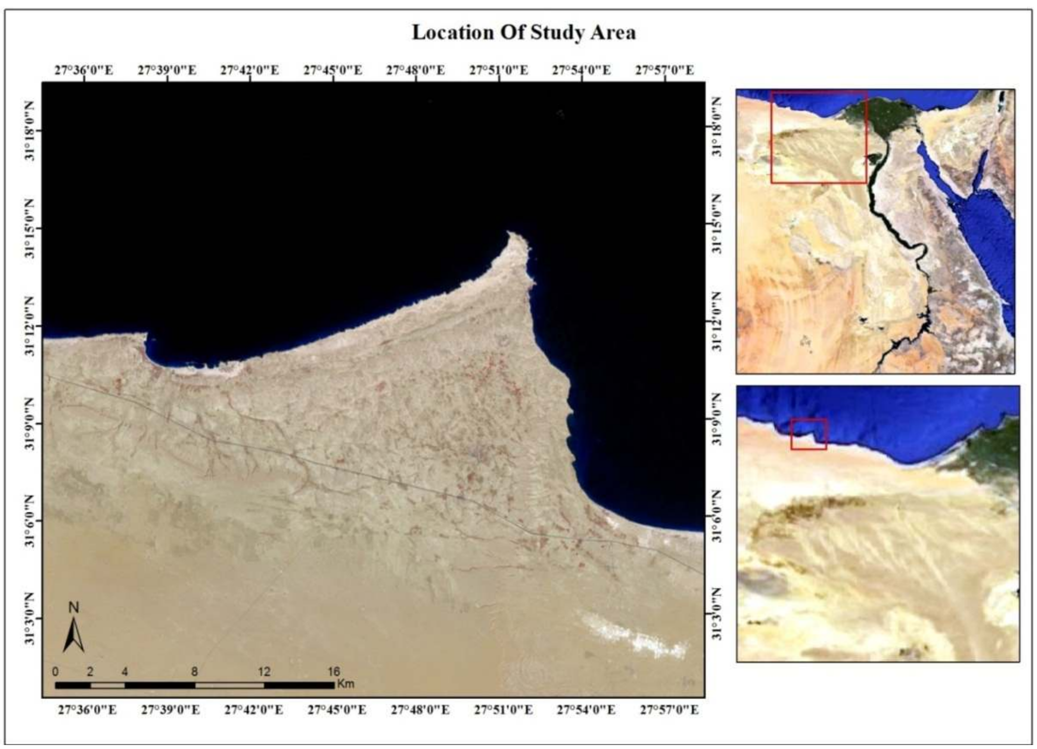

Fig. 1. Location map of the study area. Ras El-Hekma, north west of Egypt

Table 1. Details of multi resolution satallite date of acquisition and resolution

Satellite and sensors	Date of acquisition	Path/Row	Band used	Spatial resolution
LANDSAT_1 MSS	1973/05/12	192/39	Visible and NIR	60 × 60 m
LANDSAT_5 TM	1987/08/01	179/38	Visible and NIR	30 × 30 m
LANDSAT_5 TM	1995/07/06	179/38	Visible and NIR	30 × 30 m
LANDSAT_5 TM	2003/08/13	179/38	Visible and NIR	30 × 30 m
LANDSAT_8 TM	2015/08/30	179/38	Visible and NIR	30 × 30 m
Pleiades-1B	2015/08/30	179/38	Visible and NIR	0.5 × 0.5 m

perform their own geometric correction on Landsat imagery, other researchers use the correction level offered by USGS [6,7]. For most Landsat TM imagery, the United States Geological Survey (USGS) offers imagery at Standard Terrain Correction Level 1T2. This correction level implies that the imagery has been absolutely corrected using ground control points (GCPs) and a digital elevation model (DEM). The resulting products are thought to be free from distortions related to the sensor and satellite anomalies or Earth characteristics. In this study, all images are acquired from land sat satellites which According to Metadata documentation all images are orthorectified products to Standard Terrain Correction Level 1T and performed no addition geometric corrections on the imagery. They are indeed in the Universal Transverse Mercator (UTM) projection system and the World Geodetic System (WGS84) datum. The Landsat MSS image of 1973 was resampled into 30 m to match the spatial resolution of Landsat TM and ETM+ images. It has been considered as the base data and all images have been co-registered using a first-order polynomial model with base data with 0.5 pixel Root Mean Square Error (RMSE) accuracy.

2.3.2 Radiometric correction

Radiometric restoration refers to the removal or diminishment of distortions in the degree of electromagnetic energy registered by every detector. A variety of agents can cause distortion in all values recorded for image cells. The main purpose of applying radiometric corrections is to reduce the influence of errors or inconsistencies in image brightness values that may limit one's ability to interpret or quantitatively process and analyze digital remotely sensed images. To achieve perfect radiometric correction, first, the atmospheric scattering correction was performed on the images using the dark-object subtraction method to correct any atmospheric interference caused by haze, dust or smoke [8]. Fig. 2; (Fig. A) illustrate study area before atmospheric correction, (Fig. B) illustrate study area after applying the dark-object subtraction method. Then, the current radiometric correction is implemented in one step using radiometric correction tool in ENVI software, which combines the sun, view angle effects and the sensor calibration with the atmospheric correction. The required parameters (sun elevation, satellite viewing angle, and offset/gain,) are involved with Landsat metadata documentation.

2.4 Methodology

The overall methodology adopted for shoreline extraction, change rate and future shoreline prediction in this study are described in following steps and shown flow chart in Fig. 3.

2.4.1 Shoreline detection

The shoreline detection is a complex process due to the presence of water saturated zone at the land-water boundary [9]. thresholding band ratio technique has been used in president study, which uses two conditions of Band 2/Band 4 and Band 2/Band 5 for producing binary image(1) [10]. Then, the histogram threshold based on band 5 was used to develop binary image no. 2. After that, multiplying the two 2 binary image (1 by 2) to produce the image no. 3. Finally, the last step includes converting raster to vector for extracting the shoreline.

2.4.2 EPR Model for Shoreline change rate calculation

Shoreline changes and change rates can be used as an indicator for shifting in shoreline locations and direction movements.it can be defined by quantifying the amount of shoreline shift along proposed transects. After detecting the shorelines, the change rate of shoreline along parts of study area was calculated using the Digital Shoreline Analysis System (DSAS) version 4.0.1 extension for ArcGIS® [11]. In present study, EPR model has been used to

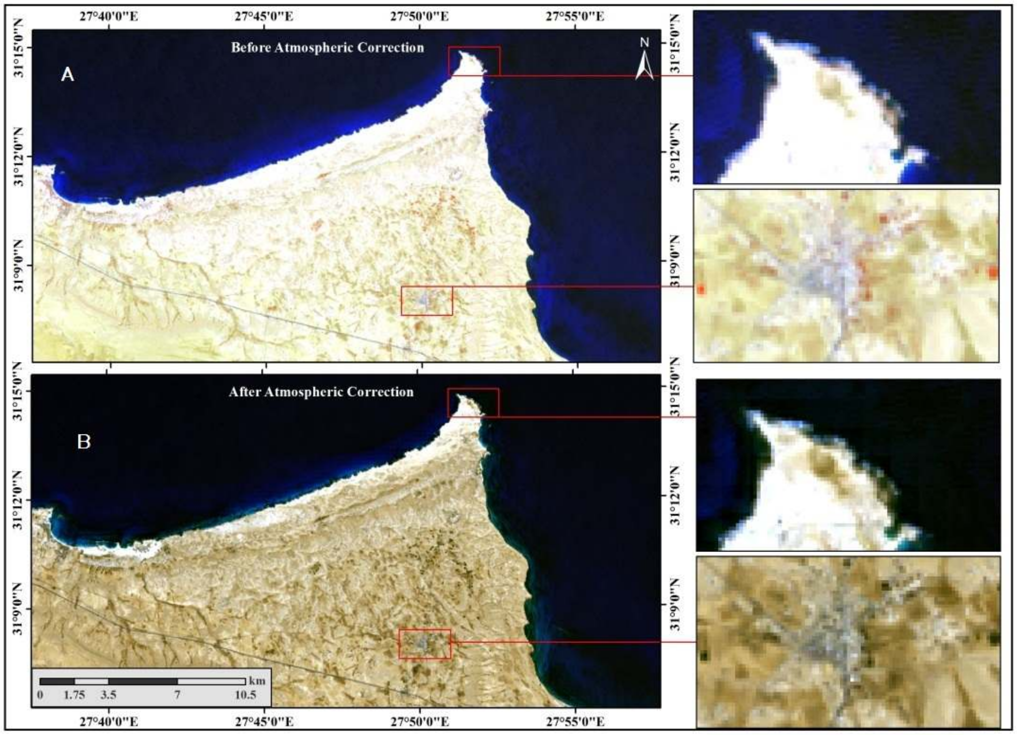

Fig. 2. A: Study area image before atmospheric correction, B: Study area image after atmospheric correction

detect change rate and predict future position of shoreline of Ras El-Hekma. Shoreline change rate is calculated relative to a baseline, Fig. 5 Baseline was constructed offshore and parallel to general trend of deferent shorelines. About 172 Transects with a spacing of 300 m apart are used for estimating the different shoreline change rates Fig. 6. According to the baseline, offshore shift (Accretion) of shoreline along with transect was considered as positive value, while landward (erosion) shift is considered negative value.

2.4.3 EPR Model for shoreline prediction

There are several methods used for predicting the future position of shoreline based on time function, a rate of deposition and erosion or sea-level rise like non-linear mathematical models [12]. Among them, End Point Rate (EPR) and Linear Regression (LR) models are the best simple and useful ones, the EPR model was adopted in this study for predicting future shoreline positions. The position of future shoreline for given data was estimated using the rate of shoreline movement (change rate), time interval between observed and predicted shoreline and model intercept which can be expressed as:

Future Shoreline position = time interval *change rate + Intercept

If Y was used to denote predicted shoreline positions

X for time interval / date

BEPR for model intercept

And m_{EPR} for the rate of shoreline change, then the equation can be written as:

$$Y = m_{EPR} * X + B_{EPR}$$

Shoreline change rate for a given set of samples, m_{EPR} calculated as:

$$m_{EPR} = (Y2-Y1) / (X2-X1)$$

Where Y_1 and Y_2 are positions of earliest and most resent shoreline position

X1 and X 2 are time interval / date for earliest and most resent shoreline

EPR intercept calculated as:

$$B_{EPR} = Y_1 - (m_{EPR} * X_1) = Y_2 - (m_{EPR} * X_2)$$

After detection shorelines from 1973,1987, 1995,2003 and 2015 images are segmented into 250 m interval and the location of a midpoint of each segment are sampled for the entire 43 km Ras El-Hekma shoreline. The DSAS (digital shoreline analysis system) has been used to calculate m_{EPR} of each sample point. Initially, the model was calibrated based on 1973 and 2003 shoreline sample and the rate of change (m_{EPR}) was calculated to predict shoreline of 2015. Also, the shorelines of the study area were predicted for short-term (2020) and long-term (2050). In order to evaluate predicted shoreline 2015, it was compared with actual shoreline which detected from a high resolution 2015 image (Pleiades). The positional shift in the predicted (future shoreline of 2015) was validated with respect to the actual image (extracted shoreline of 2015). The validation (location error in model predicted shoreline) was carried out in the term of RMSE [13]. The location errors (x and y) at each sample point was calculated then the RMSE is estimated.

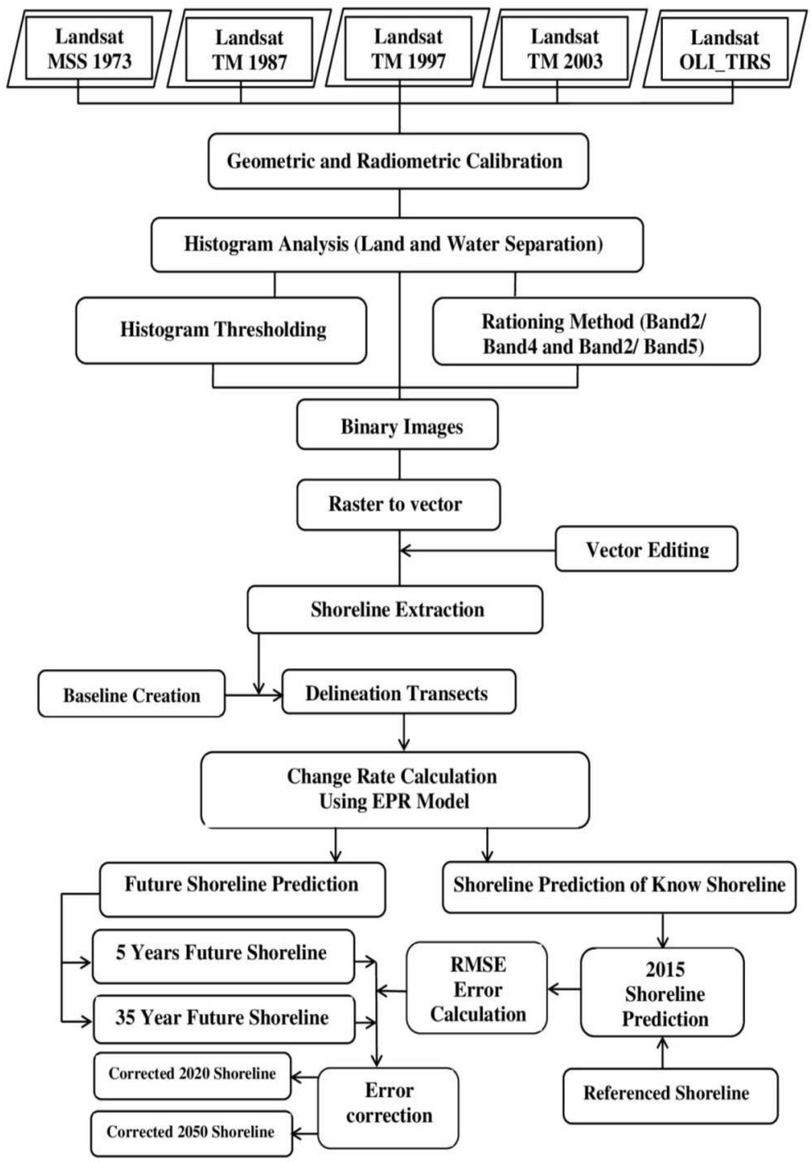

Fig. 3. Methodology framework for extraction, change rates and prediction of Shoreline

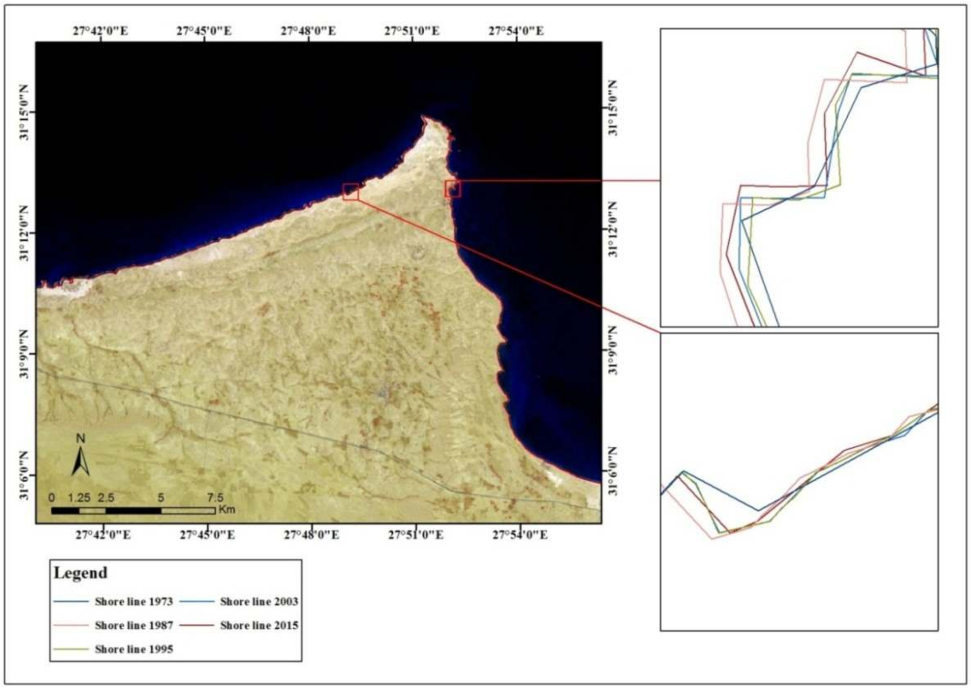

Fig. 4. Extracted Shoreline in different periods

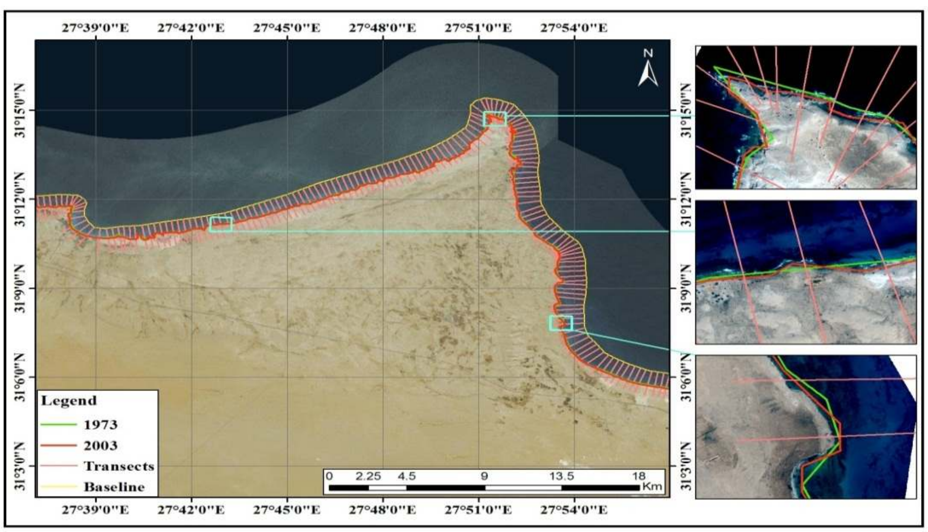

Fig. 5. Offshore baseline, transects perpendicular to shoreline and baseline

2.4.4 Model validation and predicted shoreline correction

In order to validate the EPR technique, two shorelines were compared, first is an actual shoreline (which extracted from a high resolution image) and second is the predicted one which was predicted via previous data. The Root Mean Square Error (RMSE) was estimated between the predicted and actual shoreline positions. Root Mean Square Error (RMSE) was estimated for validation, comparison and estimating error of the technique output using an equation:

$$RMSE= \sqrt{\frac{1}{n}\sum_{n=1}^{n} \ (Xpre - Xacu)^2 + (Ypre - Yacu)^2}$$

Where X pre and Y pre is coordinates of predicted shoreline at transects.

Xacu and Yacu are coordinates of actual shoreline at transects.

And n is transect numbers. After RMSE estimation the correction of predicted shorelines can be done. According to shift in (x,y) positions, actual and predicted shoreline at same time, correction rate for x and y defend as :

$$\text{Correction rate of } \mathbf{X} = \frac{\text{X acu}-\text{Xpre}}{\text{time intervale}} \quad (1)$$

$$\text{Correction rate of } \mathbf{Y} = \frac{\text{Y acu}-\text{Ypre}}{\text{Time intervale}} \quad (2)$$

Where X pre and Y pre are the coordinates of the predicted shoreline at transects.

X_{acu} and Y_{acu} are the coordinates of actual shoreline at transects.

Time interval is the time between date of predicted shoreline and most recent one.

This Correction rate can be used to adjustment the prediction shorelines as follow:

$$\text{Corrected } X_{preadj} = X_{pre} + \text{Correction rate of X} * \text{Time interval} \quad (3)$$

$$\text{Corrected } Y_{preadj} = Y_{pre} + \text{Correction rate of Y} * \text{Time interval} \quad (4)$$

Where corrected X_{preadj}, Y_{preadj} are the corrected coordinates of a predicted shoreline.

3. RESULTS AND DISCUSSION

3.1 Shoreline Changes in Ras El-Hekma during the Period 1973 – 2015

The shoreline of the Ras El-Hekma has been detected from multitemporal satellite imageries of different years (1973, 1987, 1995, 2003 and 2015). Thresholding band ratio has been used for shoreline extraction. Change rate method that is used here is EPR (End point Rate).In all, 5 shoreline positions were extracted for change detection. The Change rates calculated for the every period between 1973-2015 and then illustrated in charts (Fig. 7). The results show that there is a difference in change rate from the west where the first transect (1) to east where the last transect (166). According to charts (7-a,b,c,d and 7- e) eastern side of study area tend to erosion all the time period . The western area from transects 1 to 95 have about 40- 70% erosion and 30-60% accretion depend on the date. Overall between 1973-2015 the maximum rates are ranged from 12 m/year to -9.65 m/year where negative values represent erosion and positive values represent accretion. The minimum, maximum and average change rates for different dates are illustrated in table (1). The average rates are defended from -0.8 to -4.25 for erosion and 0.54 to 1.60 for accretion definitely not high.

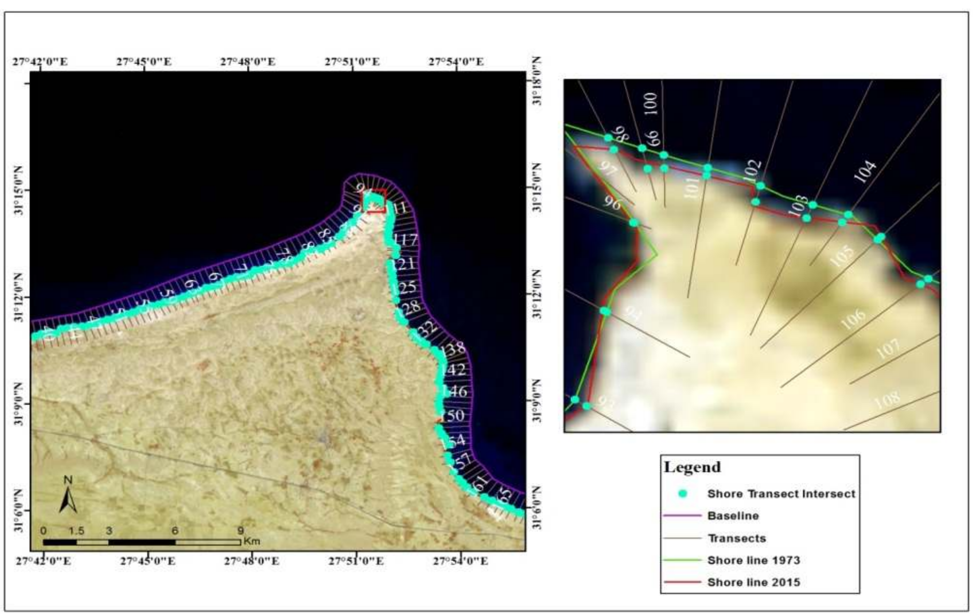

Fig. 6. Transect numbering from west to east along the coast of Ras El-hkma

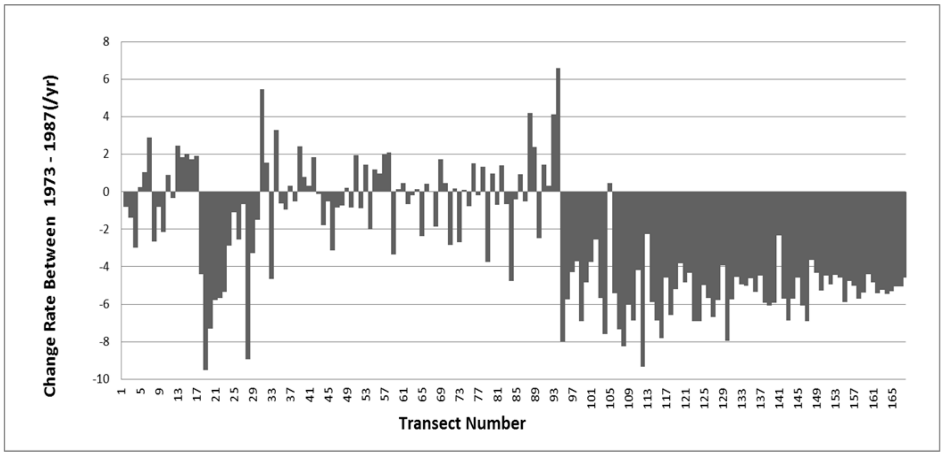

Fig. 7a. Shoreline change rate between 1973-1987 (m/y)

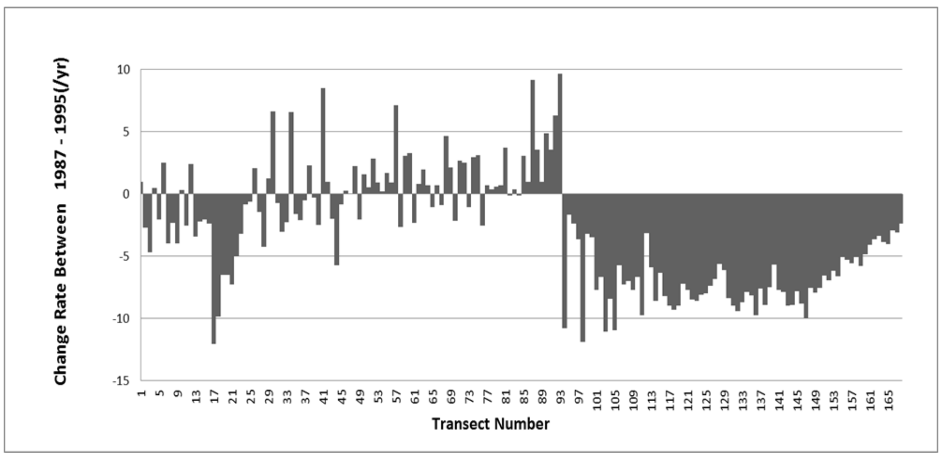

Fig. 7b. shoreline change rate between 1987-1995 (m/y)

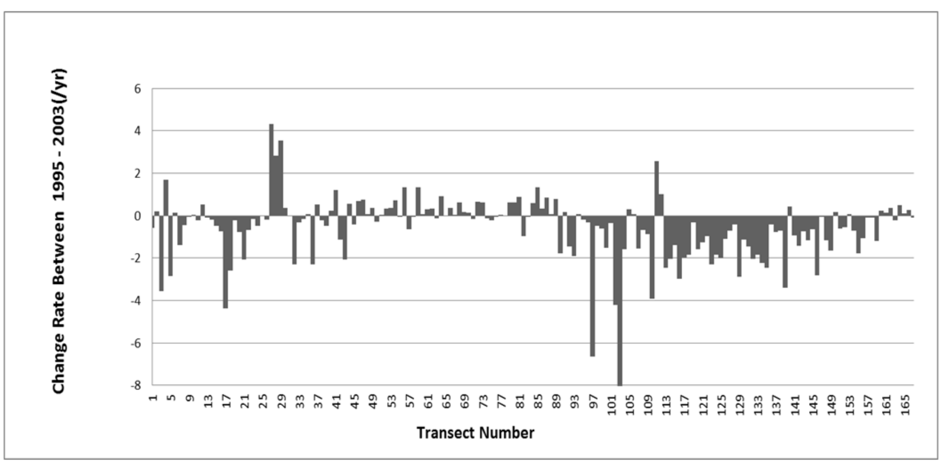

Fig. 7c. Shoreline change rate between 1995-2003 (m/y)

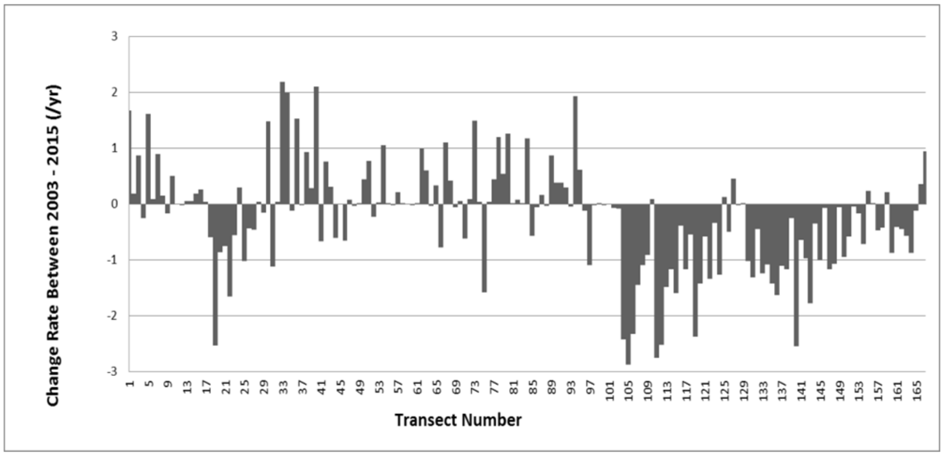

Fig. 7d. shoreline change rate between 2003-2015 (m/y)

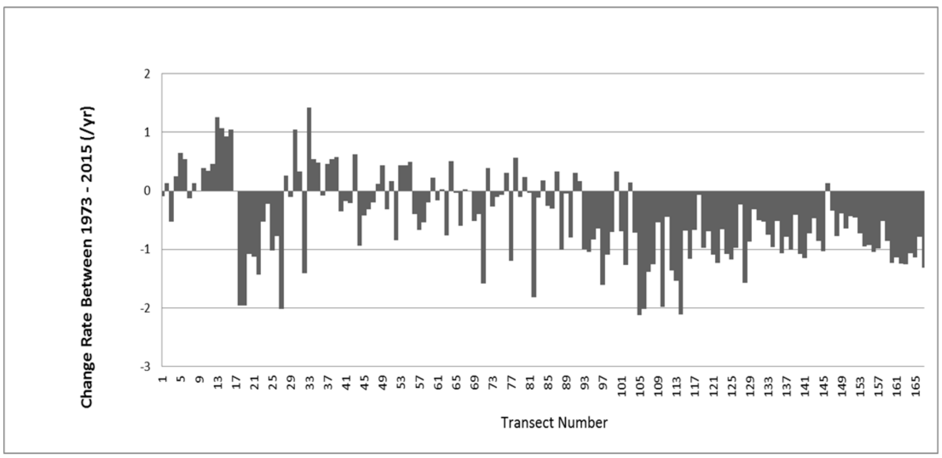

Fig. 7e. Shoreline change rate between 1973-2015 (m/y)

Table 2. Statistics of shoreline change rates in different time interval (1973-2015)

	Year/(m/y)	**1973-1987**	**1987-1995**	**1995-2003**	**2003-2015**	**1973-2015**
Change rate (erosion)	Max	9.50	9.65	8.35	2.87	2.12
	Min	0.01	0.06	0.01	0.01	0.01
	Mean	4.25	2.65	1.26	0.8	0.80
	Year (m/y)	**1973-1987**	**1987-1995**	**1995-2003**	**2003-2015**	**1973-2015**
Change rate (accretion)	Max	6.61	12	4.32	3.19	1.42
	Min	0.04	0.11	0.02	0.01	0.02
	Mean	1.6	5.5	0.7	.054	0.45

3.2 Future Shoreline Prediction Using EPR Model

EPR technique has been used for predicting future shoreline of this study area in short term 2020 and long term 2050, Fig. 8. The predicted shorelines in short and long term indicate that the deposition and erosion in Ras El-Hekma at all transects will be small in the future. The average erosion will be -4.80 m between 2015- 2020 and average accretion will be 2.60 m. The maximum erosion will be observed in the easting part of

Ras El-Hekma with -14.1 m between 2015- 2020 at transect No.114. Also, the maximum accretion will be observed in western part with +8.75 m at transect No.14 for the same dates.

3.3 Validation of EPR model and Future Shoreline Correction

The change rate of shoreline calculated from shoreline position in 1973 and 2003, according to this rate, the predicted shoreline of 2015 was detected. To evaluate The End Point Rate (EPR) model the estimated shoreline was compared with the actual shoreline extracted from high resolution image 2015. Displacements between sample points (x,y) results from the intersection of actual and predicted shoreline 2015 have been estimated. This displacement or positional shift at each sample points is illustrated in the Fig. 9. The positional error varies from -49.8 m to 76.3 m. It has been found that model prediction error is homogeneous in the all of the shorelines. The overall error (RMSE) for the future predicted shoreline2015 was found to be 15.75 m (RMSE). The correction error procedure was applied for 2020 and 2050 shorelines then the corrected shorelines plotted Fig. 10.

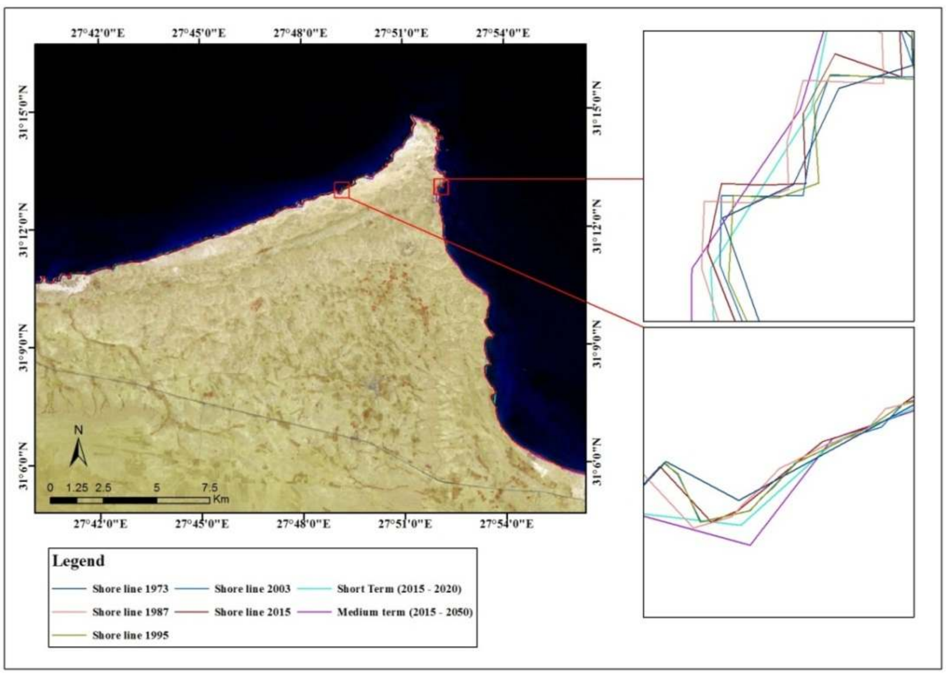

Fig. 8. All shorelines 1973,1987,1995,2003,2015 and Predicted 2020, 2050 shorelines

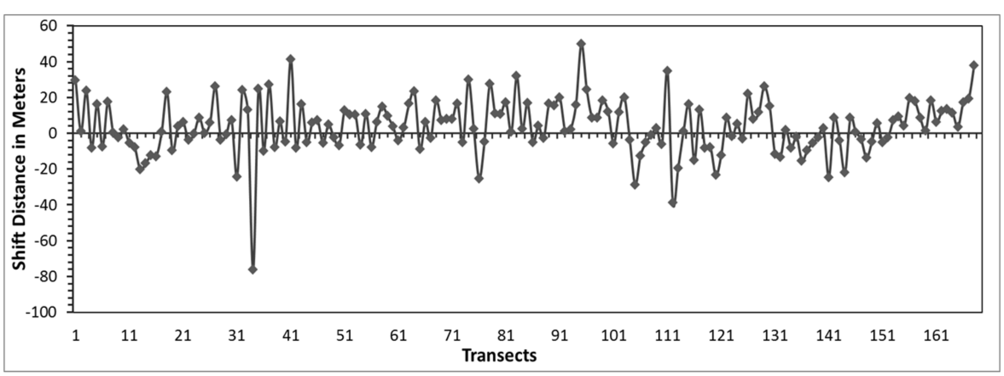

Fig. 9. Error in positions of points between predicted shoreline and actual shoreline at 2015

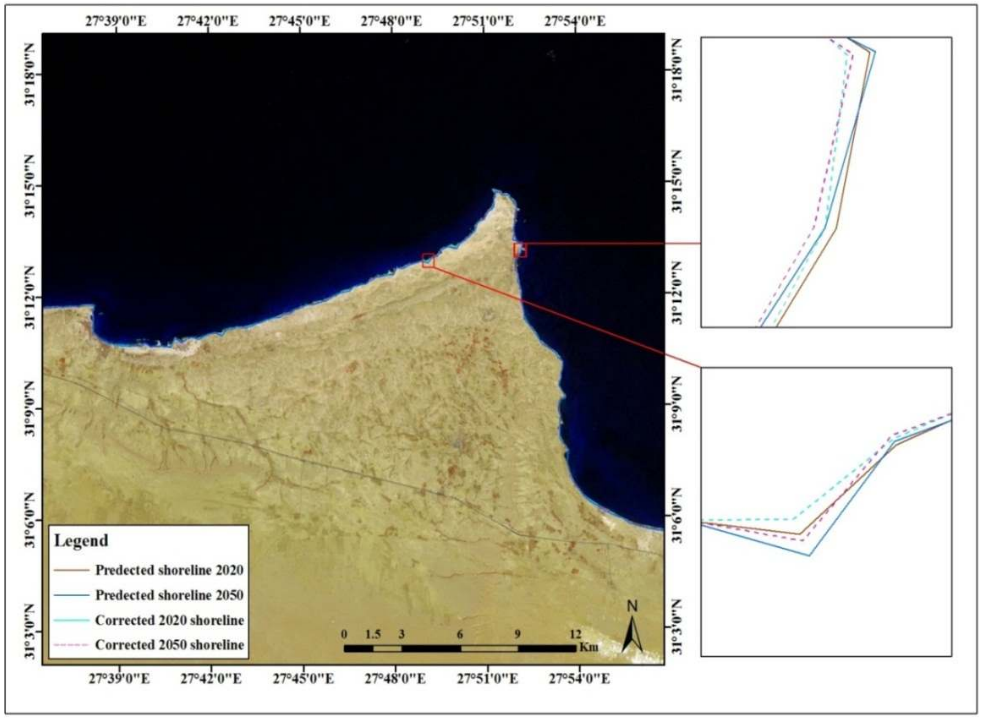

Fig. 10. Predicted 2020, 2050 shorelines and its correction

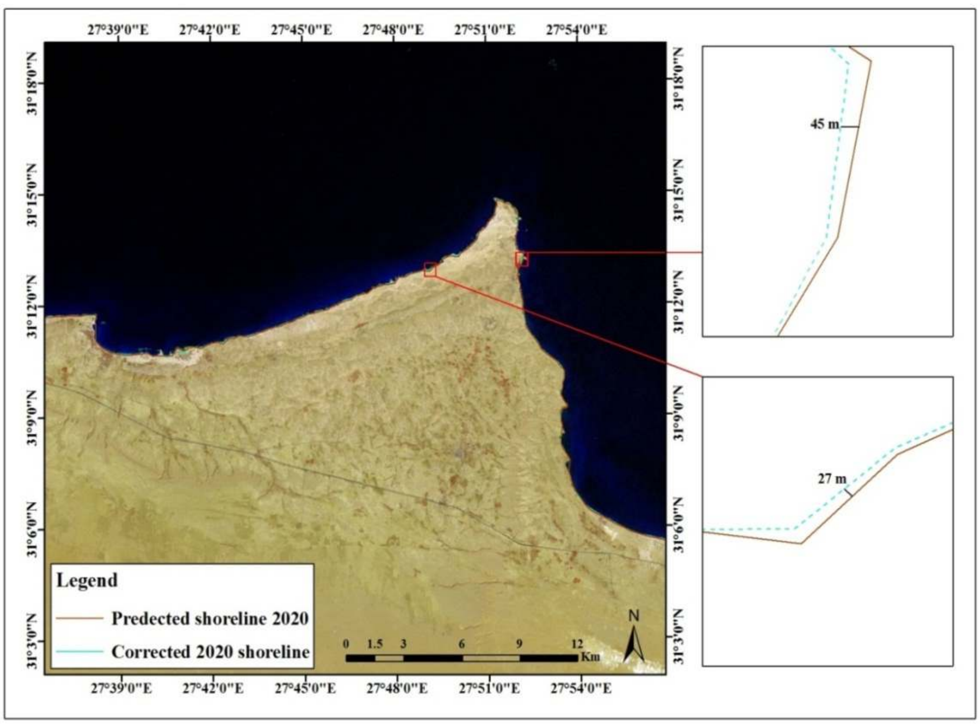

Fig. 10a. Predicted 2020 shoreline and its correction

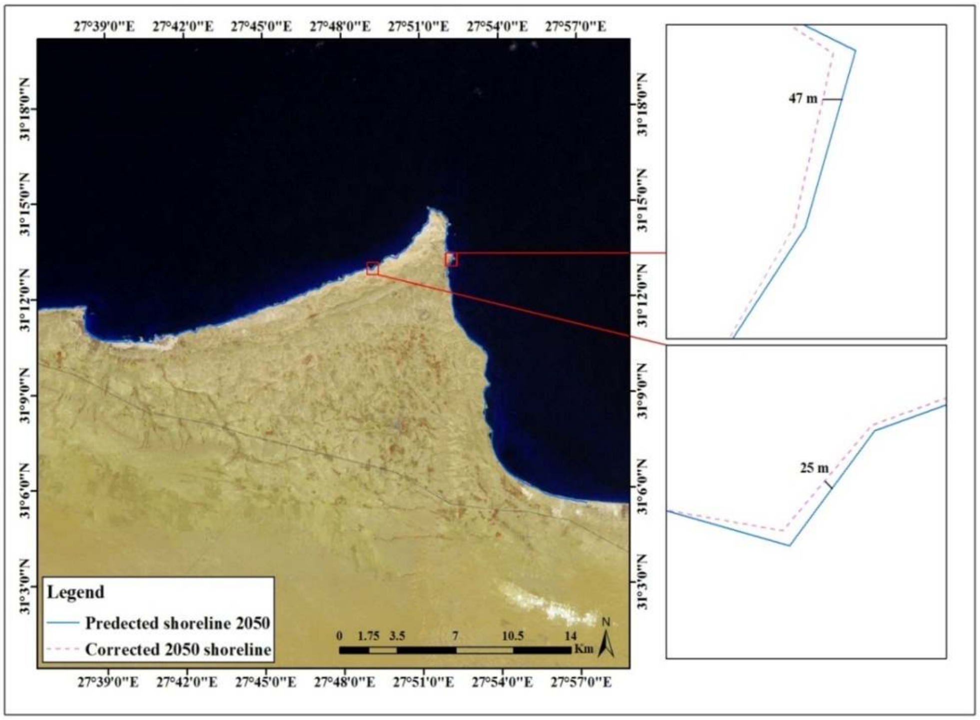

Fig. 10b. predicted 2050 shoreline and its correction

4. CONCLUSION

Extraction, change detection and the future prediction of shorelines have been investigated in this dissertation for Ras El-Hekma coastal area using land sat images representing 42 years period, acquired in 1973, 1987, 1995, 2003 and 2015. To extract shorelines for these dates the band ratio thresholding method (b2/b4 and b2/b5) has been used. Endpoint rate (EPR) technique has been used to detect the change rate and future prediction. Comparing two shorelines for the same date (2015) gives an ability to estimate Rote Mean Square Error (RMSE). First one is an actual shoreline (extracted from a high resolution image) and the second is a predicted shoreline which was predicted using the previous history data. Root Mean Square Error (RMSE) was estimated between the actual and the predicted shoreline sample positions. After that, the correction for future predicted shoreline can be done. Change rate results of this dissertation show that eastern coastal area of Ras El_Hekma is only an erosional area on another hand the western coastal area has a variable behavior in erosion and accretion. Using the 2003 - 2015 results as a reference, Accretion rates is ranged from 0.01 m/year to 3.19 m/year with an average 0.05 m/year while erosion rates were between 0.01 to 2.87 m/year with an average of 0.80 m/year. Both rates are significantly low compared with 106 m/year occurred as average rate of shoreline along Rosetta Promontory, north of Egypt between 1971 and 1990 [14].

COMPETING INTERESTS

Authors have declared that no competing interests exist.

REFERENCES

1. Lillesand TM, Kiefer RW, Chipman JW. Remote sensing and image interpretation. 15th ed. USA.704: John Wiley and Son; 2004.
2. De Jong, Steven M, Freek D, Van Der M. Remote sensing image analysis: Including the spatial domain Kluwer Academic Publishers. MA, USA. 2004;359.
3. Miao GJ, Clements MA. Digital signal processing and statistical classification. Artech House Inc. MA. USA. 2002;414.
4. Winarso G, Budhiman S. The potential application of remote sensing data for coastal study. Proc. 22nd. Asian

Conference on Remote Sensing, Singapore; 2001.
5. Malarvannan S, Kannan J. Assessment of shoreline changes over the Northern Tamil Nadu Coast, South India using Web GIS techniques. Coastal Conservation; 2016. DOI: 10.1007/s11852-016-0461-9
6. Li B, W Yu, J Wang. An analysis of vegetation change trends and their causes in Inner Mongolia, China from 1982 to 2006. Advances in Meteorology Article. 2011;1-8.
7. Yang L, Xian G, Klaver JM, Deal B. Urban land-cover change detection through sub-pixel impervious mapping using remotely sensed data. Photogrammetric Engineering & Remote Sensing. 2003;69(9):1003-1010.
8. Louati M, Saidi H, Zargouni F. Shoreline change assessment using remote sensing and GIS techniques: A case study of the Medjerda delta coast, Tunisia. Arab. J. Geosci; 2014. DOI: 10.1007/s12517-014-1472-1
9. Maiti S, Bhattacharya AK. Shoreline change analysis and its application to prediction: A remote sensing and statistics based approach. Mar Geol. 2009;257:11–23.
10. Niya AK, Alesheikh AA, Soltanpor M, Kheirkhahzarkesh MM. Shoreline change mapping using remote sensing and GIS. Int. J. Remote Sens. Appl. 2013;3:102–107
11. Himmelstoss EA. DSAS 4.0-Installation Instructions and User Guide. In: Thieler ER, Himmelstoss EA, Zichichi JL, Ergul A, Eds. The Digital Shoreline Analysis System (DSAS) Version 4.0—An ArcGIS Extension for Calculating Shoreline Change. US Geological Survey Open-File Report 2008-1278, ver. 4.2. 81.
12. Li R, Liu J, Felus Y. Spatial modelling and analysis for shoreline change and coastal erosion monitoring. Marine Geodesy. 2001;24:1-12.
13. Paine J, Morton R. Shoreline and vegetation line movement, Texas gulf coast 1974 to 1982. The University of Texas at Austin, Bureau of Economic and Geology and Geological Circular. 1989;89:1-50.
14. Ali M, Kazuo N, Abdelazim N, Moheb I. Detection of shoreline and land cover changes around Rosetta promontory, Egypt, based on remote sensing analysis. Land. 2015;4:216-230. DOI: 10.3390/land4010216

Peer-review history:
The peer review history for this paper can be accessed here:
http://sciencedomain.org/review-history/18320